XXXVI Ibero-Latin American Congress on Computational Methods in Engineering
CILAMCE
Rio de Janeiro, 22-25 Nov 2015

DYNAMIC MODEL FOR AN EVAPORATOR OPERATING WITH R-1234yf AND R-134a

Thiago Ali

thiagoali@hotmail.com

Willian Moreira Duarte

willianmoreiraduarte@gmail.com

Graduate Program in Mechanical Engineering (PPGMEC) of the Federal University of Minas Gerais, Av. Antônio Carlos, 6627, Belo Horizonte, MG, CEP 31270-901

Philippe Haberschil

philippe.haberschil@insa-lyon.fr

Centre d'Energétique et Thérmique de l'INSA de Lyon (CETHIL), Bâtiment Sadi Carnot 9, rue de la Physique, INSA de Lyon, Campus La Doua, LyonTech, 69621, Villeurbanne, Cedex, France

Antônio Augusto Torres Maia

aamaia@ufmg.br

Graduate Program in Mechanical Engineering (PPGMEC) of the Federal University of Minas Gerais, Av. Antônio Carlos, 6627, Belo Horizonte, MG, CEP 31270-901

Luiz Machado

luizm@demec.ufmg.br

Graduate Program in Mechanical Engineering (PPGMEC) of the Federal University of Minas Gerais, Av. Antônio Carlos, 6627, Belo Horizonte, MG, CEP 31270-901

Abstract. *The production and trade of CFCs fluids have been regulated since 1987, when the Montreal Protocol was signed. Since then, the refrigeration industry has been developed researches in fluids with characteristics favorable to the environment. In recent years, the fluid R-1234yf (low levels of ODP and GWP) has been used to replace the traditional fluid R-134a in automotive air conditioning systems in Europe and USA. This paper presents a mathematical model of an evaporator of a refrigeration machine operating with the fluids R-134a and R-1234yf. The mathematical model was based on the principles of conservation of energy, mass, and linear-momentum. Correlations obtained from literature were used to calculate the heat transfer, pressure drop and void fraction. To validate the model, 36 tests were carried out in a experimental testing bench operating with R-134a as refrigerant fluid.*

Results obtained with the mathematical model were satisfactory when compared with the experimental results. Furthermore, operation simulations of the evaporator were carried out to compare the behavior of the system operating with the fluids R-134a and R-1234yf.

Keywords: *Dynamic model, Evaporator, Refrigeration system, R-1234yf, R-134a*

1 INTRODUCTION

In the early 30s, chlorofluorocarbons (CFCs) were introduced in refrigeration and in other applications, for example, aerosols. It was believed at that time that these fluids were safe and harmless to the environment. However, Molina and Rowland in 1977 showed hypotheses linking the damage to the ozone layer to the action of CFCs in the atmosphere. Since then, many discussions around the theme happened and in 1987 an agreement named Montreal Protocol (UNEP, 1997) was signed by 24 countries and the European Economic Community to regulate the production and trade of OSD's (Ozone Depleting Substances). Later in the Helsinki Conference (1989) and at the London Conference (1990), other countries started to follow the Montreal Protocol recommendations. Years later in Kyoto, Japan, a new agreement named Kyoto Protocol was also signed by several countries (UNFCCC, 1997). In this agreement it was proposed to reduce the emission of greenhouse gases effects that enhances global warming. These events were divided lines in the refrigeration history and boosted the use of different chemicals such as hydrochlorofluorocarbons (HCFCs), hydrofluorocarbons (HFCs), inorganic compounds, zeotropic and azeotropic mixtures. Such substances cause less harm than to that caused by CFCs.

There are two indices that have often been used to investigate the destructive influence of refrigerants in nature. The ODP (Ozone Depletion Potential) is a number that refers to the amount of ozone which is destroyed by a substance. The ODP is the ratio between the impact caused by certain chemical compound when compared to the impact caused by a similar amount of R- 11. The ODP of CFC's and HCFC's have a value from 0.01 to 1.0, while for mixture which take the Bromine (Br) in its composition the amount may exceed 10 points. The GWP (Global Warming Potential) is a number that refers to the contribution to global warming that a particular substance causes. The GWP is the ratio between the warming caused by a certain substance when compared to the heating caused by a similar amount of CO_2 mass (Dinçer, I. and Kanoglu 2010). In this sense, research and development has occurred to replace conventional refrigerants for substances with more favorable characteristics to the environment. Currently a new generation of refrigerants has been most commonly used in refrigeration processes; they are the HFO's that have low levels of ODP and GWP. Some of these substances are presented in Table 1.

In 2010, countries that follow the Montreal Protocol failed in reducing the production and the sale of CFCs and in 2040 it is expected the same for the HCFCs however, new recommendations such as the EU 517/20 has forced air conditioning system to abandon HFCs and adopt the HFO's because of its environmental characteristics. Refrigerants such as R-134a, R-404A and R-401a should be replaced so that systems can be adapted to the requirements of European policy. R- 134a is a fluid from the family HFC- that has been affected by the new European regulations. Therefore, many studies have been developed seeking a replacement for R- 134a. Currently two strong candidates have been outstanding, which are, HFO - 1234yf (2, 3, 3, 3 - tetrafluorpropano) and HFO- 1234ze the (E) (trans 1,3,3,3 - tetrafluorpropano) by having a physical behavior similar to that of R- 134a .

Tabela 1. – Valores de ODP e GWP de alguns fluidos refrigerantes

Refrigerant	ODP	GWP	Refrigerant	ODP	GWP
CFC-12	1	10600	R-410A	0	1730
HCFC-22	0,055	1810	R-407C	0	1530
HFC-23	0	14800	R-404A	0	3260
HFC-32	0	675	Propane	0	3
HFC-125	0	3500	Iso-Butano	0	3
HFC-134a	0	1430	CO2	0	1
HFC-143a	0	4470	HFO-1234yf	0	4
HFC-152a	0	124	HFO-1234ze(E)	0	6

Higashi and Meisei (2010) developed an experimental study about the properties of these refrigerants and various thermodynamic properties were measured. Temperature, pressure and specific critical mass, steam pressure, density, specific mass of liquid and saturated steam, specific heat at constant pressure and surface tension were determined for a wide range of temperature and pressure. In this study it was shown that the thermodynamic properties of R-1234yf and R-1234ze (E) are similar to R-134a, making them good candidates to be used as replacement fluids.

Similarly, Reasor et.al. (2010) developed a comparative study about the refrigerant fluid R-134a, R410A and R-1234yf. The thermodynamic properties of the three fluids were compared to determine the feasibility of replacing R-134a and R-R410A by 1234yf in automotive air conditioning systems or refrigeration systems. The study has concluded that the thermodynamic properties of R-1234yf are very similar to R-134a, but the same is not true for R410A. In addition, an analysis through computer simulation was conducted seeking to determine the operating performance of the three fluids working in the same heat exchanger. The simulations showed that R-134a and R-1234yf have similar results to the outlet temperature of refrigerant fluid. The pressure drop ranged from 40% into geometries tested demonstrating that more careful analysis must be made to replacement of the fluid in refrigeration systems already built.

A study by (Zilio et. Al., 2011) has conducted several experiments in a compact air conditioning system. In this study, the thermodynamic behavior of R-134a and R-1234y were compared. When operating with R-1234yf, the cooling ability and the system COP (Coefficient of Performance) were considerably smaller than the R-134a systems. However, these values can be significantly increased with some modifications in the R-1234yf systems. Numerical simulations have shown that an increase in the condenser area of 20% and 10% of the evaporator and the use of another compressor in the system can display a higher COP using the R-1234yf.

Lee and Jung (2011) also evaluated the performance of R-1234yf and R-134a in a test bench for automotive air conditioning. The tests were carried out in summer and winter conditions. The results showed that the COP and the refrigeration capacity of the R-1234yf was 2.7% and 4% lower than R-134a, respectively. The compressor discharge temperature and the refrigerant mass were 6.5ºC and 10% lower than R-134a. Based on these results the authors concluded that the R-1234yf can be used for a long period due to their favorable characteristics to the environment as well as present an acceptable performance.

Similarly, a performance analysis was held (Cho et. al. 2013) in an automotive air conditioning system charged with R-134a and R-1234yf. The internal heat exchanger was installed in order to improve cooling performance of R1234yf and to investigate the level of performance improvement in comparison with conventional R134a system. Performance test by using R1234yf and R134a in the same system showed low power consumption and cooling capacity for using R1234yf, that is, up to 4% and 7%. In particular, performance comparison between the R1234yf and R134a for automotive air conditioning revealed that cooling capacity and COP of the 1234yf system without the IHX decreased by up to 7% and 4.5%, respectively, but those with the IHX decreased by up to 1.8% and 2.9%, respectively.

Esbrí et. al. (2013), performed a study to analyze the energy performance of R-134a and R-1234yf. Comparisons are made taking refrigerant R134a as baseline, and the results show that the cooling capacity obtained with R1234yf in a R134a vapor compression system is about 9% lower than that obtained with R134a in the studied range. Also, when using R1234yf, the system shows values of COP about 19% lower than those obtained using R134a, being the minor difference for higher condensing temperatures. Finally, using an internal heat exchanger these differences in the energy performance are significantly reduced.

Recently, Babiloni et. al. (2014) developed a study to investigate some mixtures of HFCs proposals (R-32, R-135, R-134a and R-152a) and HFO's (R-1234yf and R-1234ze (E)) which would be consistent with the limits recommended by the US 517 / 20. The theoretical analysis indicated that mixtures of HFC / HFO's have a lower performance than HFCs (although the experimental study has shown otherwise) and in most cases, no restrictions on the GWP values recommended by the European standard.

Previous work has shown that the substitution of R-134a by R-1234yf in the conventional systems is less efficient. However, a study presented by Li et. al. (2014) proved the contrary when the EERC system (ejector-Expansion Refrigeration Cycle) was employed using R-1234yf. The study showed that the COP and cooling capacity of the volumetric EERC using R-1234yf reached a peak of 5.91 and 2590.76 kJ / m³, respectively. Compared with the standard refrigeration cycle the R1234yf EERC generally has a better performance, especially at the condition of higher condensing temperature and lower evaporation temperature. The COP and VCC improvements of the R1234yf EERC over the standard refrigeration cycle are also greater than that of the R134a cycle.

Different configurations of refrigeration cycle using an intermediate exchanger and an ejector-expander were also studied by Moles et. al. (2014) using R-1234yf and R-134a. The study has concluded that the most efficient configuration is one that uses an expander or an ejector-expander. On the other hand, using an internal heat exchanger in a cycle which replaces the expansion valve by an expander or an ejector could produce a detrimental effect on the COP. However, for all the configurations the introduction of an internal heat exchanger produces a significant increment on the cooling capacity.

Recently, a mathematical model was developed by Miranda et. al. (2015) for a shell and tube heat exchanger, with finned tubes, to operate with R-134a and R-1234yf. The model developed for the evaporator uses the ε-NTU method for calculating the evaporation pressure, the exit enthalpy of the refrigerant and the temperature of the secondary fluid. The model accuracy was evaluated using different correlations for the heat transfer coefficient for two-phase flows and compared to experimental data. It was found that the parameter that showed the greatest deviation between the experimental data and the model was the evaporation pressure. The simulations also showed that the overall coefficient of heat transfer to the R-1234yf was no more of 10% lower than R-134a.

As can be noted in the literature review, many studies have assessed the energy performance of R-1234yf and its suitability as substitute for R134a in a refrigeration system. In most of the considered works it was verified that the system thermal behavior was only investigated in steady state. At the time this paper is dedicated to produce a comparison between the thermal performance of a refrigeration system, operating in transient mode, employing R-1234yf and R134a as refrigerant fluid.

2 MATHEMATICAL MODEL

The mathematical model developed in this work is based on the conservation laws of mass, energy and momentum. To calculate the heat transfer coefficient, the pressure drop and the void fraction, correlations extracted from specialized literature were employed. In the development of the mathematical model, the following considerations were considered: (1) The axial heat transfer by conduction is negligible; (2) The flow of refrigerant fluid and the secondary fluid occurs only in one dimension; (3) There is no heat loss to the external environment; (4) The physical properties do not vary in the pipe cross section; (5) The fluid potential energy is negligible. The resolving methodology consists in dividing the evaporator into *n* control volumes. In each element, the equations (1), (2) and (3) were applied to determine the flow properties of the refrigerant fluid.

$$A_f \frac{\partial}{\partial t}[\rho_f(h_f - P_f v_f)] = -A_f \frac{\partial}{\partial z}(G_f h_f) + \alpha_f p_f(T_p - T_f) \tag{1}$$

$$\frac{\partial \rho_f}{\partial t} + \frac{\partial G_f}{\partial z} = 0 \tag{2}$$

$$\frac{\partial}{\partial z}\left\{P_f + G_f^2\left[\frac{x^2 v_v}{\alpha} + \frac{(1-x)^2 v_l}{1-\alpha}\right]\right\} = -\frac{\partial G_f}{\partial t} - \left(\frac{dP}{dz}\right)_F - g\rho_f sen(\theta) \tag{3}$$

To determine the temperature in each control volume, it was written the equations of energy conservation for the secondary fluid and the pipe wall. These expressions are represented by Eq. (4) and (5).

$$\rho_a A_a c_{pa} \frac{\partial T_a}{\partial t} = -G_a A_a c_{pa} \frac{\partial T_a}{\partial z} - \alpha_a p_a(T_a - T_f) \tag{4}$$

$$\rho_p A_p c_{pp} \frac{\partial T_p}{\partial t} = \alpha_a p_a(T_a - T_p) - \alpha_f n_t\, p_f(T_p - T_f) \tag{5}$$

In Eq . (1) to (4) A_f, ρ_f, h_f, P_f, v_f, G_f, α_f, p_f, T_f, e T_p are respectively cross section area, the specific mass ($kg.m^{-3}$), the enthalpy ($J.\ kg^{-1}$), the pressure (Pa), the specific volume ($m^3.kg^{-1}$) , the mass flux ($kg\ m^{-2}\ s^{-1}$), the heat transfer coefficient ($W\ m^{-2}\ K^{-1}$), the perimeter (m), the refrigerant fluid and the wall temperature (K) in each element. In equation (3) x, v_l, v_v, α, g, e $(dP/dz)_F$ refer respectively to the vapour quality, the specific volume of liquid and saturated steam ($m^3.kg^{-1}$), the void fraction, the gravity acceleration ($m\ s^{-2}$) and pressure drop (Pa). The subscripts *a*, *p*, and *f* are related to the water, the tube wall and the refrigerant fluid.

2.1 Heat Transfer Correlation

The refrigerant flows through the tubes changing phase as it receives heat from the secondary fluid. The heat transfer process by convection was modeled using heat transfer correlations for monophasic and biphasic flow depending on the state of the fluid in each element. Initially the fluid enters in the evaporator as a mixture (liquid + steam) and the heat transfer coefficient can be estimated by the correlation of Dengler and Addoms (Turaga , 1985), as shown in Eq.(6).

$$\alpha_{bf} = C\left(\frac{1}{\chi}\right)^n \alpha_l \tag{6}$$

The coefficients C and *n* in Eq.(6) are 3.5 and 0.5 respectively. The variables χ and α_l represent the Martinelli parameter, and the heat transfer coefficient by convection for the liquid phase, given by the correlation presented by Dittus - Boelter (Incropera et.al., 2008). During the flow the tube inner surface becomes increasingly drier due to the phenomenon of evaporation. With the disappearance of the fluid film on the surface, the heat transfer coefficient decreases while the quality assumes a critical value that can be estimated by the correlation Sthapak (Koury , 1998), as presented by Eq.(7).

$$x_{crit} = 7.943\left[Re_v\left(2.03x10^4 Re_v^{-0.8}\left(T_p - T_{sat}\right) - 1\right)\right]^{-0.161} \tag{7}$$

In Eq.(7), Rev, Tp, Tsat, represent the Reynolds number for steam phase, the surface temperature and the saturation temperature. After the dry wall region, the heat transfer coefficient was estimated by a 3rd polynomial to keep the function continuity.

2.2 Pressure Drop Correlations

To estimate the pressure drop in the the two-phase flow region it was employed the correlation proposed by Lockhart and Martinelli (Eq. 8) (Machado 1996). The correlation proposed by Fanning was used for the single phase flow (Ozisic , 1985) .

$$\left(\frac{dP}{dz}\right)_F = \left(\frac{dP}{dz}\right)_{vs} \phi_{vs}^2 = \frac{f_{vs} v_v G}{2d_{int}} \phi_{vs}^2 \tag{8}$$

$$\left(\frac{dP}{dz}\right)_F = \frac{f v G}{2d_{int}} \tag{9}$$

The friction factor *f* can be estimated using Eq. (10), (11) e (12).

$$f = \frac{64}{Re} \qquad Re < 2300 \tag{10}$$

$$f = \frac{0.316}{Re^{0.25}} \qquad 2300 < Re < 80000 \tag{11}$$

$$f = 0.0054 + \frac{0.3964}{Re^{0.3}} \qquad Re > 80000 \tag{12}$$

2.3 Void Fraction

The specific mass of the refrigerant fluid reduces as the fluid receives heat from the secondary fluid. For this work the specific mass was calculated by Eq. (13) that uses the void fraction α to determine the steam and liquid portion in each element.

$$\rho_f = \rho_l + \alpha(\rho_v - \rho_l) \tag{13}$$

In Eq. (13) the subscripts *1* and *v* refer to the specific density of the liquid and saturated steam locally. The void fraction in this case is calculated by correlation Zivi (Rice, 1987) given by Eq. (14).

$$\alpha = \frac{1}{1+\frac{(1-x)}{x}\left(\frac{\rho_v}{\rho_l}\right)^{2/3}} \tag{14}$$

2.4 Compressor Model

To develop the compressor model presented in this work, it was not considered (1) The pressure drop in the valves; (2) The mass flow rate variations at the inlet and the outlet of the compressor; (3) the heat exchange between the compressor and the surroundings. At the compressor outlet, the mass flow rate estimation was performed using Eq. (15).

$$\dot{m}_3 = NV\rho_{f2}\eta \tag{15}$$

Where N, V, ρ_{f2} e η *are* the rotational speed, the piston displacement volume, the specific mass at the compressor inlet and the volumetric efficiency. The compressor volumetric efficiency is estimated by Eq. (16),

$$\eta = 1 + c - c\left(\frac{P_{out}}{P_{in}}\right)^{c_v/c_p} \tag{16}$$

where c, P_{out}, P_{int}, c_v and c_p are the clearance ratio, the discharge pressure, the suction pressure, the constant volume and constant pressure specific heats.

2.5 Flowchart Model evaporator

The evaporator model works in conjunction with the compressor model. First, an evaporation pressure value is estimated and the physical properties such as pressure, temperature, specific density, enthalpy and others are locally determined through Eq. (1), (2) and (3). In the last element the mass outflow of the compressor is compared with the mass flow of the evaporator outlet. In the case of these values exceed the predetermined error, is used then the Newton-Raphson convergence method for estimating a new evaporation pressure value until the difference between the compressor outflow and the evaporator is lower than that previously established. After the calculation of the pressure the temperature of the walls and the secondary fluid are also calculated using the Newton-Rapshon. Figure 1 represents the flowchart for the calculation model described.

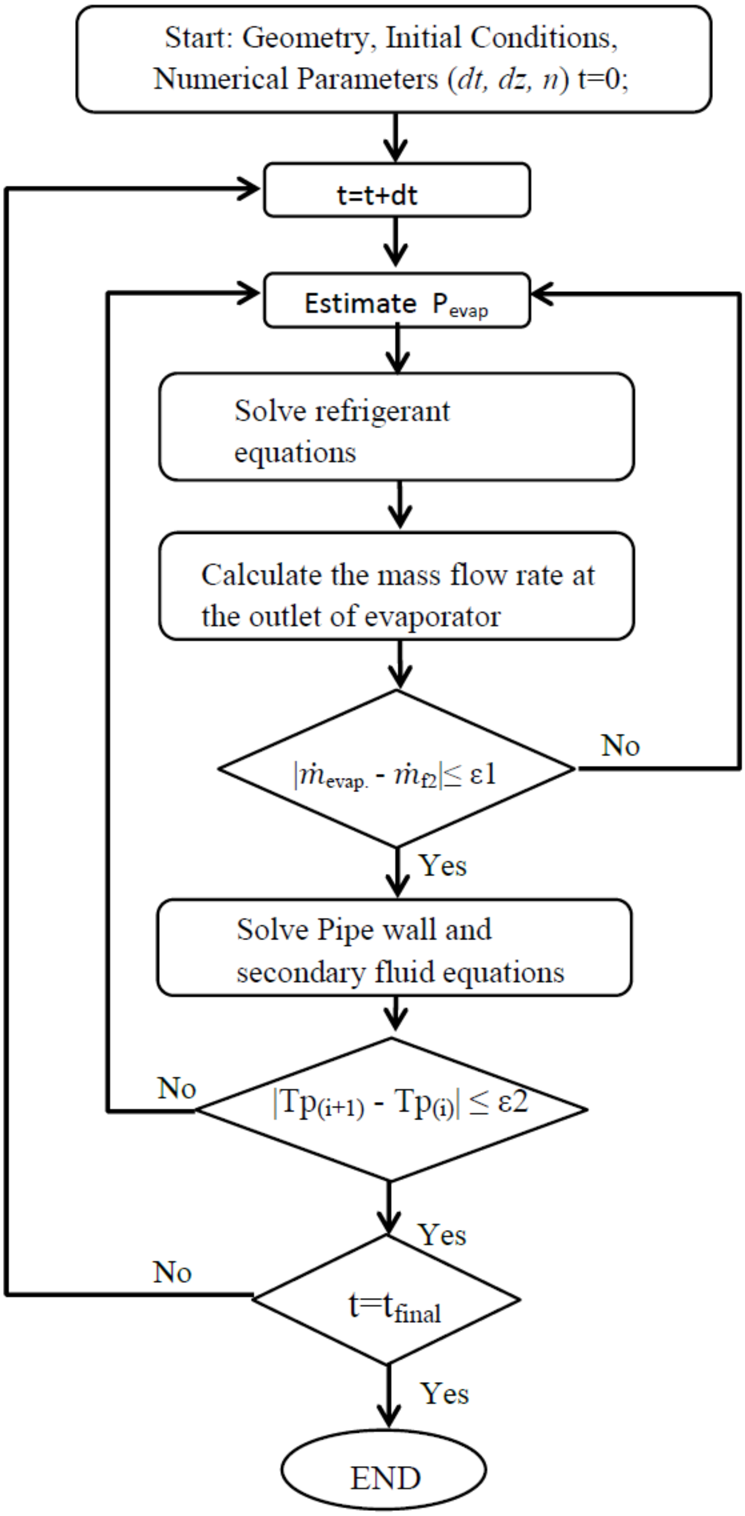

Figure 1. System Model fluxogram

4 MESH TEST

A mesh test (Fig. 2) was conducted to determine the minimum number of elements required to have a consistent answer from the numercal model. The simulations presented in Fig. 2 were performed in steady state, with a refrigerant fluid initial mass of 80 g and a mass flow rate of 70 kg / h. The water flow rate and the water inlet temperature were respectively 0.68 m³ / h and 20 °C. The expansion device was considered isenthalpic and the sub cooling was of 5°C. As noted, the minimum number of elements required for a consistent response with a variation of ± 0.2 °C is 150 elements. Simulations with a number of elements inferior to 150 may yield inconsistent results despite the convergence of the numerical method. Instead, simulations performed with a superior number of elements provided satisfactory results with numerical precision, however, a very refined mesh requires more computational effort and time to be processed with no equivalent improvements in the results. This study used 400 elements to discretize the evaporator.

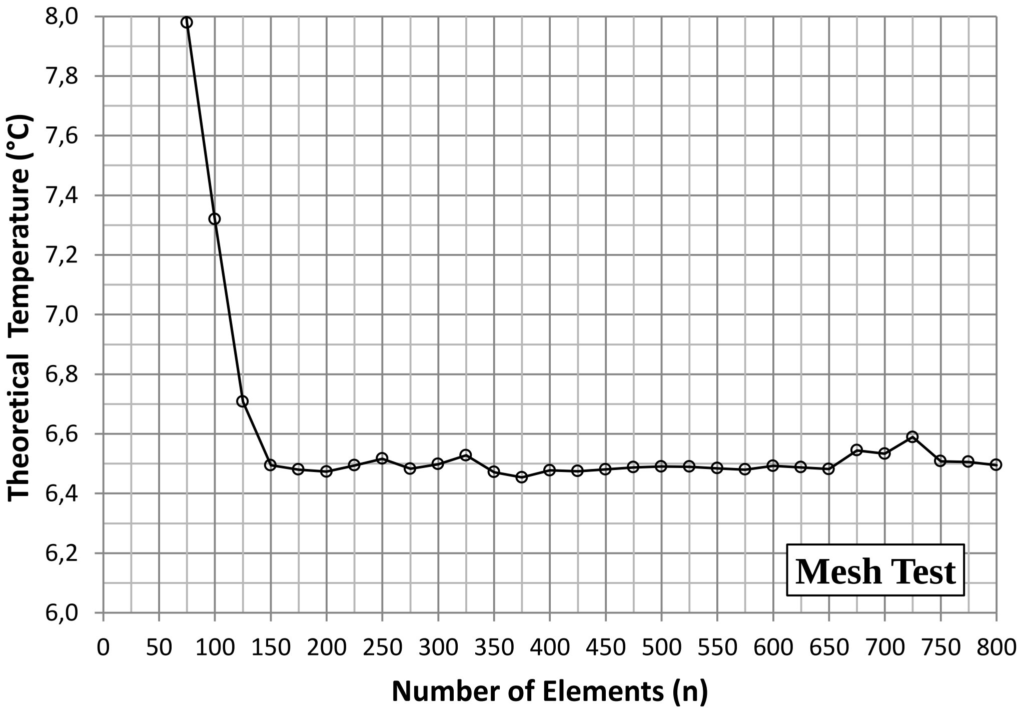

Figure 2. Mesh Test

For this work it was adopted a step time of 0.5 s for the range $50 \leq t \leq 60$ and a step time of 1 s for the remaining operating instants.

5 VALIDATION

The numerical model validation was performed using experimental data obtained from the test bench presented in Fig. 3. During the experiments, the test bench was loaded with R-134a as the refrigeration fluid and pure water as secondary fluid in the evaporator and condenser. The condenser is shell and tube type and the condensation temperature of the R-134a depends on the water temperature at the condenser inlet. This temperature is adjusted by mixing warm water, originating from the condenser itself, with room temperature water, coming from the feeding system. To validate the evaporator model, the condensing temperatures used were 45ºC, 50ºC and 55ºC.

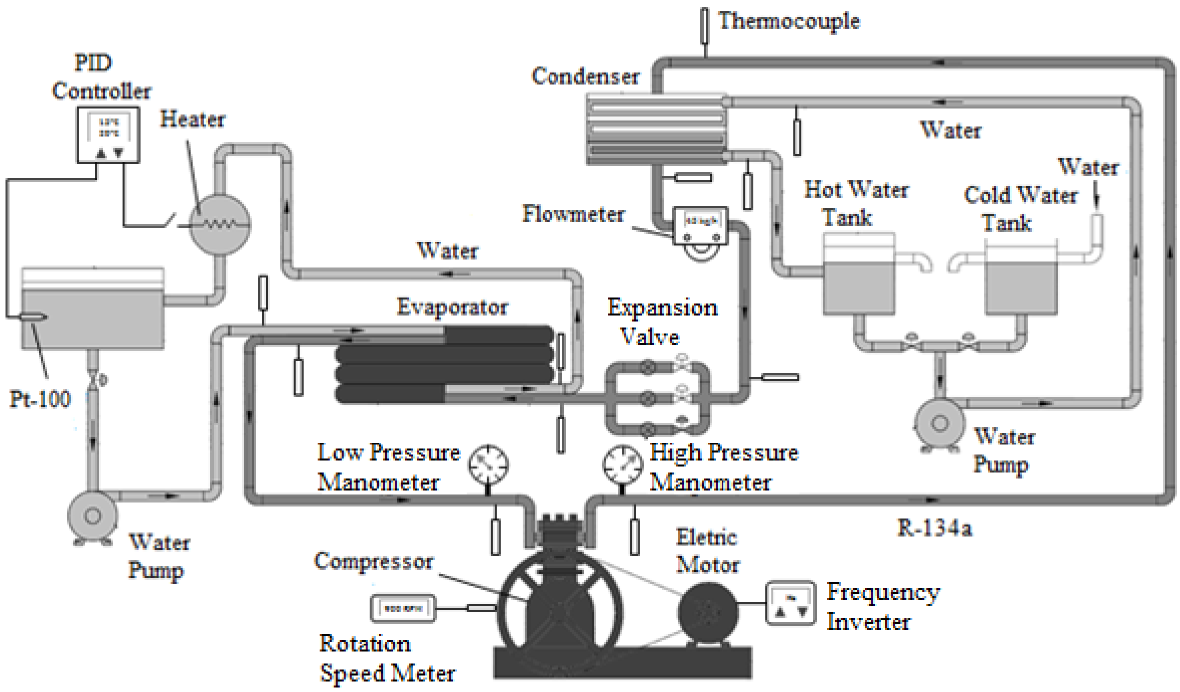

Figure 3. Scheme of the test bench and measurement instruments.

The evaporator is coaxial type and it consists of an envelope tube of flexible PVC and three inner copper tubes through which the refrigerant fluid flows. The water circulates in counter flow in the annular space between the cooper tubes and the PVC tube. In the evaporator, the secondary fluid temperature is kept within the desired limits by an electrical heating system. By controlling the water inlet temperature it is possible to adjust the evaporating temperature. To validate the evaporator model, the evaporating temperatures used were -5ºC, 0ºC, 5ºC and 10ºC.

It was performed a set of 36 tests for different operating conditions. Due to the presence of a condensation trap at the compressor inlet, the Eq. (17) was used to estimate the temperature at the evaporator outlet (T_{f2}), as a function of the temperature at the outlet of the condensation trap (T'_{f2}).

$$T_{f2} = T'_{f2} - \frac{(U\,S\,\Delta T_{MLDT})}{\dot{m}_f\,c_p} \tag{17}$$

Where U, S, ΔT_{MLDT}, c_p are the overall heat transfer coefficient, the area of heat exchange, the logarithmic average temperature difference, the specific heat of the refrigerating fluid, respectively. The product $U{\times}S$ was calculated when the system was operating with a compressor speed of 1000 rpm and an evaporation temperature of 0 °C. These operational settings correspond to an intermediate operating condition of all the tests performed in this work. Assuming that the heat transfer coefficient of air is much lower than the heat transfer coefficient of refrigerant is reasonable to consider that the $U \times S$ value remains constant for the other tests. By proceeding in this way, the simulated points could be corrected in the mathematical model and validated with experimental data. Figure 4, 5 and 6 presents a comparison between the theoretical and experimental evaporation temperature, for the compressor speed of 900, 1000 and 1100 rpm. As can be seen in Fig. 4, some of the theoretical data deviates more than ± 2 °C when the compressor is running at 900 rpm and when the evaporating temperature was below to 0 °C. The same results can be observed for compressor speed of 1000 and 1100 rpm in Fig. 5 and 6

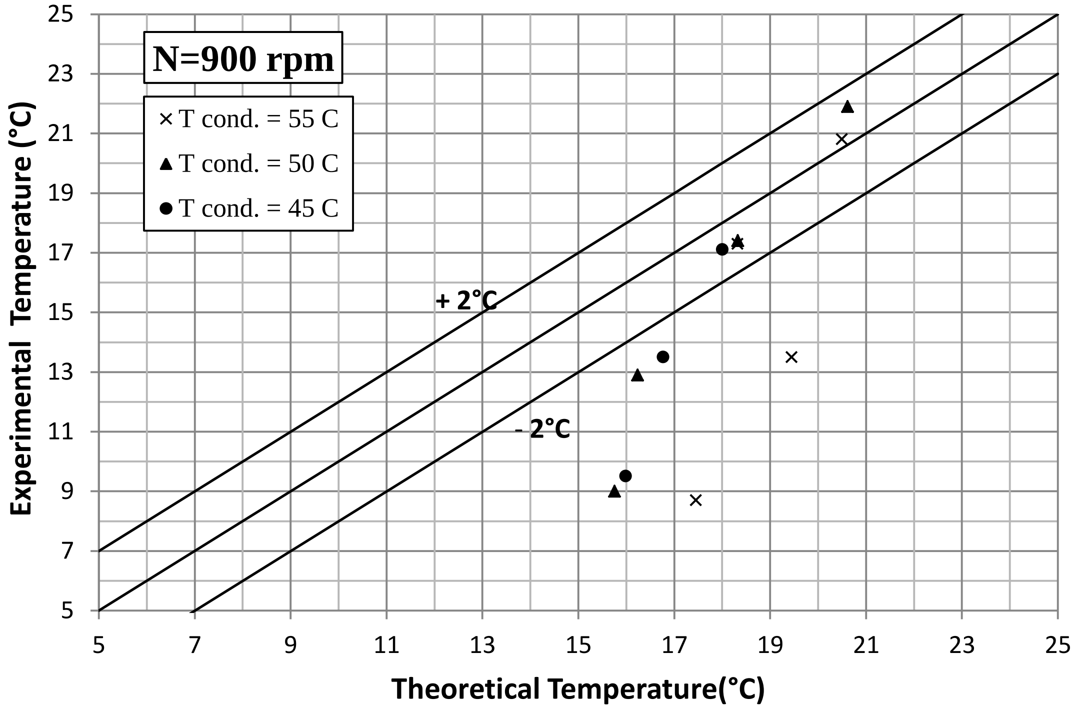

Figure 4. Deviation between Model and Experimental Data, N=900 rpm

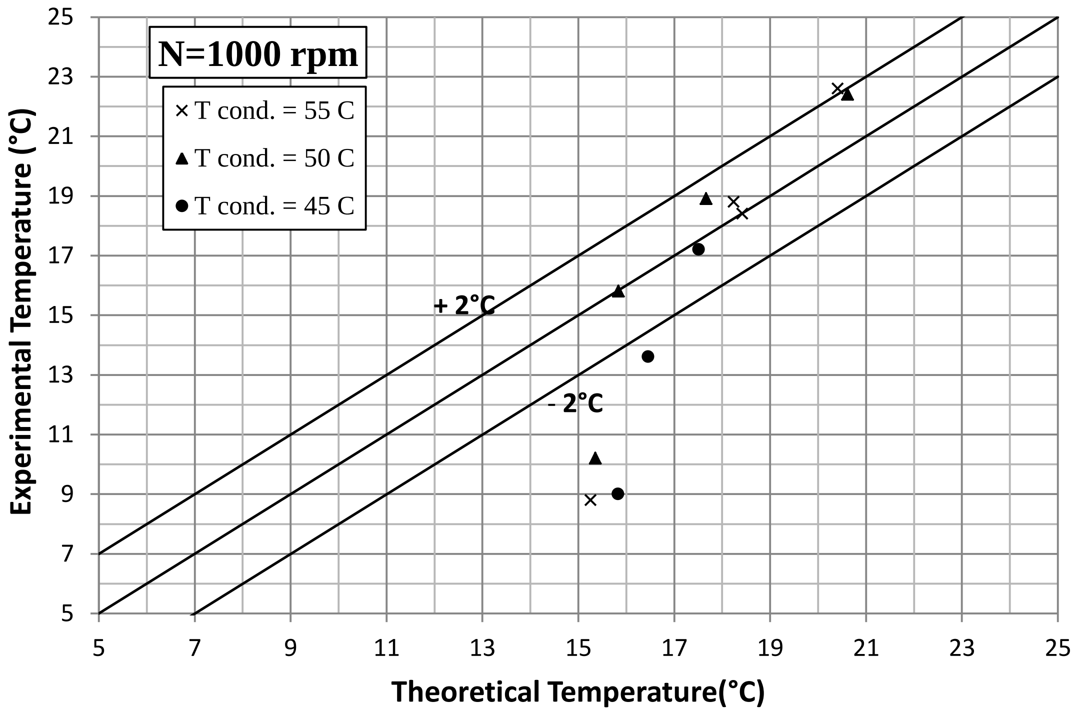

Figure 5. Deviation between Model and Experimental Data, N=1000 rpm

As can be seen the deviation decreases when the rotation is increased and the condensation temperature. The results show that the model can predict the evaporation temperature of ± 2 ° C with an error range when the evaporation temperature is above 0 ° C. However, new tests should be conducted to evaporation temperatures below this limit. In addition, a new validation for the rotation of 900 rpm.

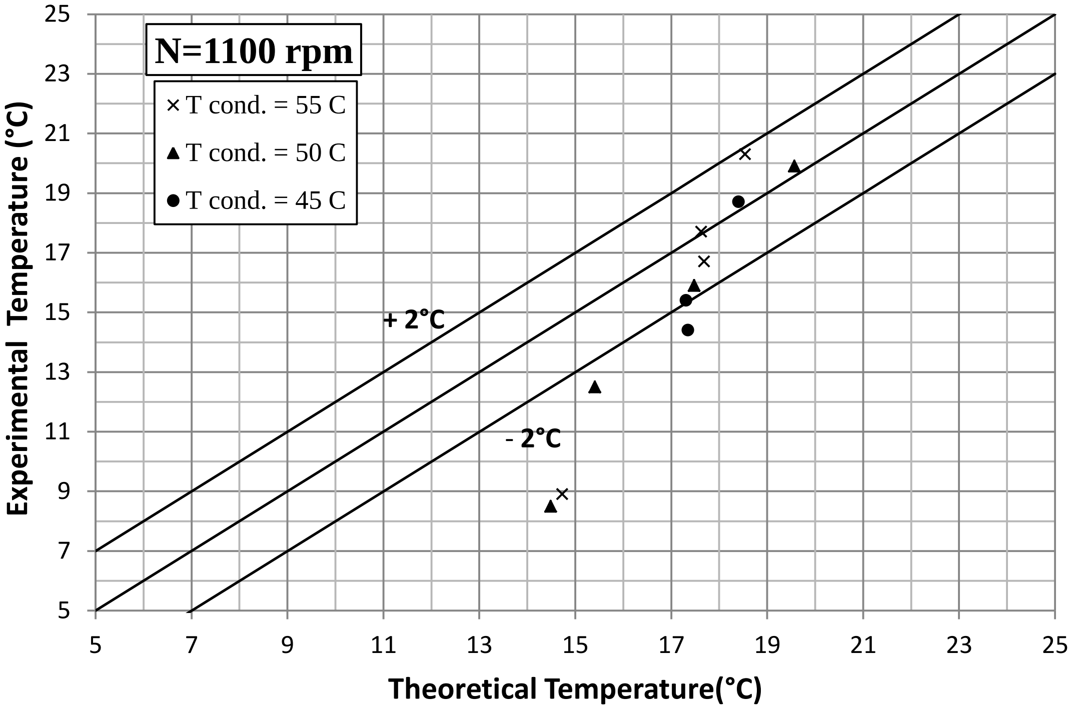

Figure 6. Deviation between Model and Experimental Data, N=1100 rpm

6 RESULTS AND DISCUSSION

6.1 Numerical Simulation for Transient Regime

The transient numerical simulations consisted of first obtaining the theoretical steady-state initial point. This point was obtained using a high step time (10^7 s). Then, the mass flow rate at the inlet of the evaporator was reduce by 5%. The response generated by the mathematical model is presented in Figure 7. The step perturbation was performed when t=50 s. Since the latent heat of vaporization R1234yf is less than that of R134a, the evaporation temperature reached for R1234yf (8.8 ºC) is greater than the evaporation temperature reached for R134a (6.4 °C). In the range from 50 to 250 s, the evaporation temperature decreases until it reaches a new level. The reduction in temperature is accompanied by a reduction in the mass of refrigerant fluid inside of the evaporator. This reduction is caused by the unbalance between the mass flow rate at the inlet and the outlet of the evaporator.

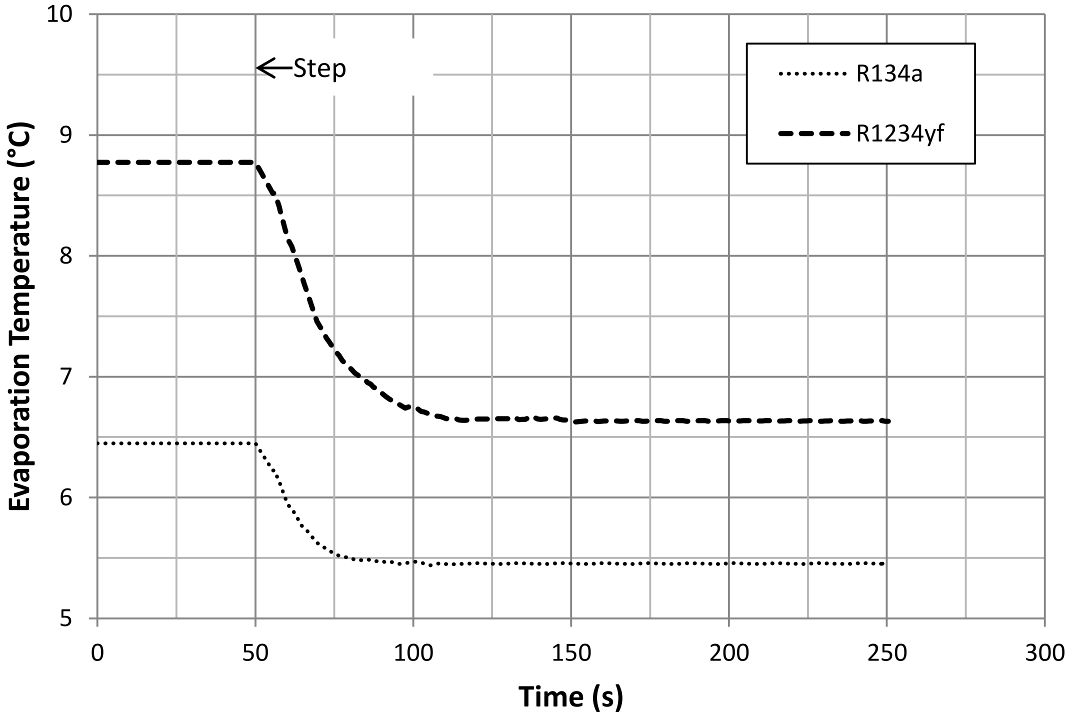

Figure 7. Degree in the Temperature Evaporation

Figure 8 shows the mas flow rate at the inlet of the evaporator ($\dot{m}_{f,in}$) and the mass flow rate at the outlet of the evaporator for both refrigerating fluids. As can be observed, after a 5% of reduction in the mass flow rate at the inlet of the evaporator, the outlet mass flow rate decreases slowly until it reaches the steady state. The area between the curve for each fluid and the mass flow rate at the inlet of the evaporator represents the mass of refrigerant fluid that was removed from the evaporator. After the step perturbation, the variation in the evaporation temperature of the R1234yf is higher than the R134a. This is because of the amount of mass removed from the evaporator when it was working with R1234yf is greater than when it was working with R134a, as can be seen in Fig. 8.

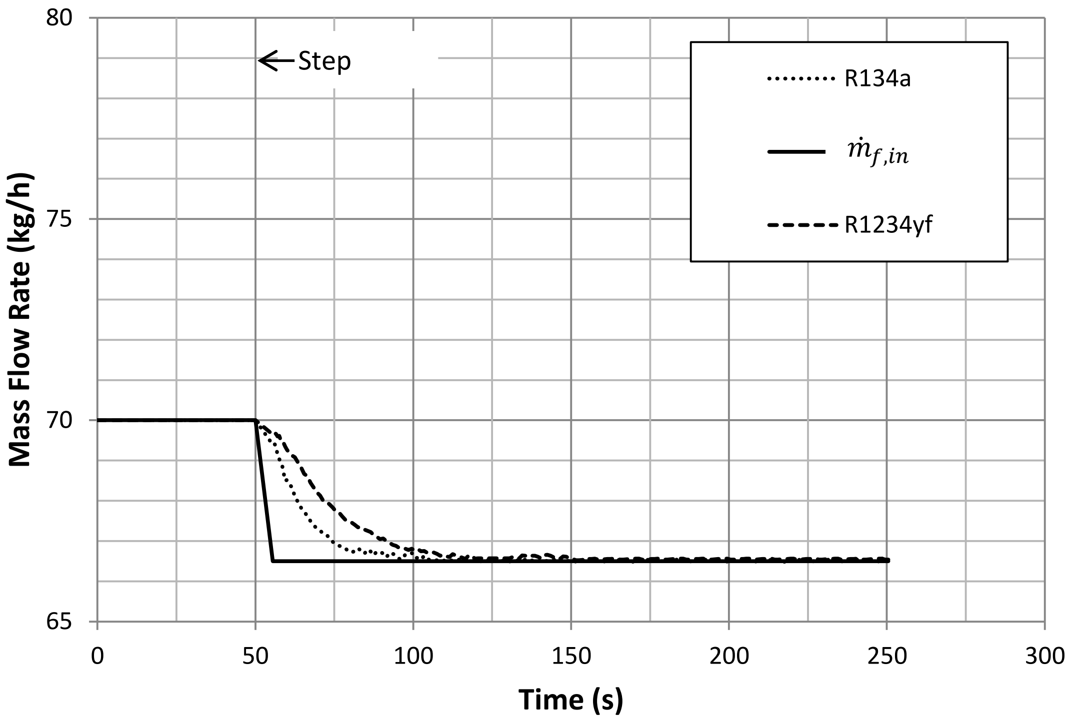

Figure 8. Degree in the Inlet Flow

After the step perturbation, the time required for the evaporator to reach a new steady state is associated with the time constant. The two fluids have very similar physical properties, though the heat transfer coefficient for R1234y is smaller than R134a as shown in Fig. 9. Because of this difference the thermal resistance of R1234yf fluid stabilizing the temperature

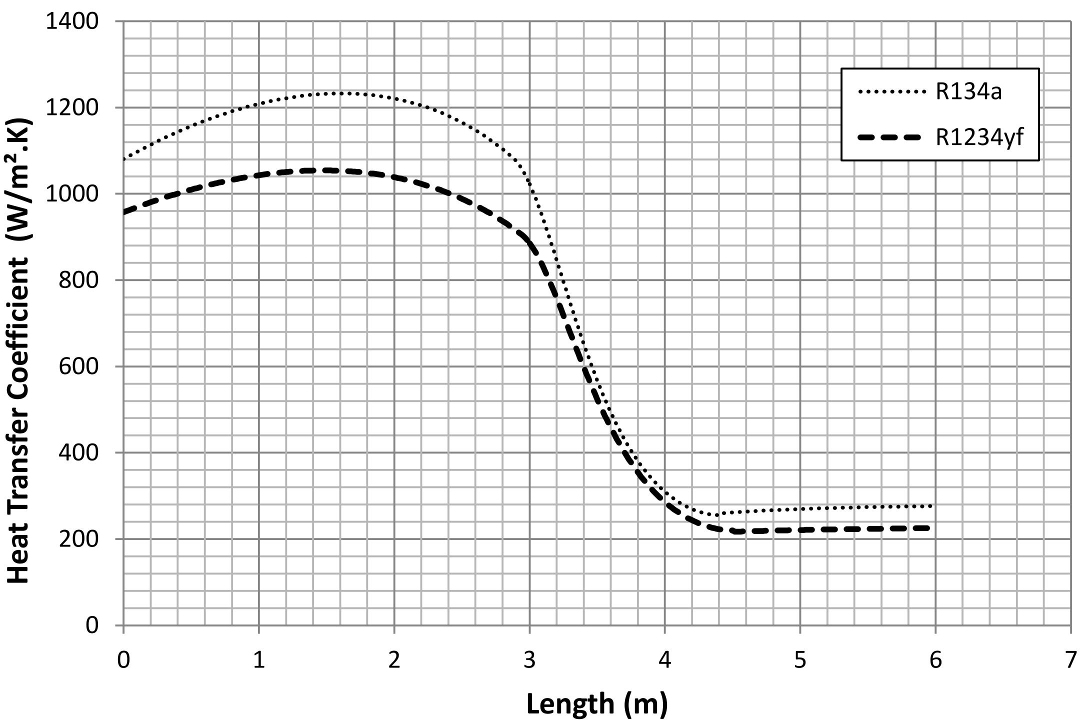

Figure 9. Comparing Heat Transfer Coefficient of R134a and R1234yf

is increased.

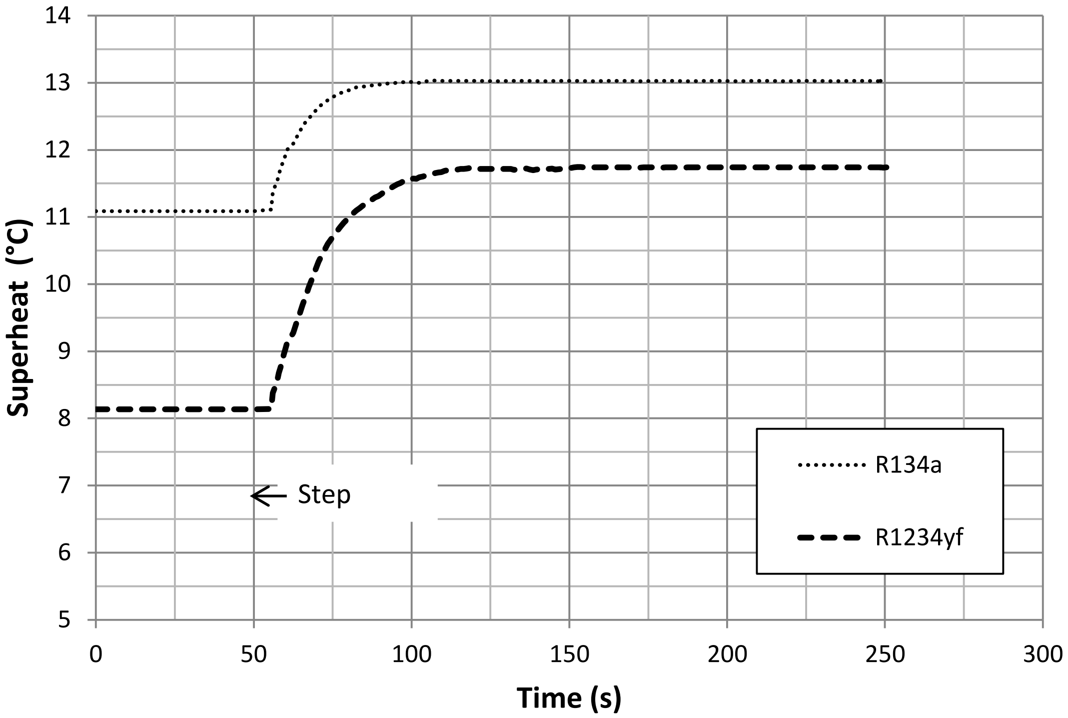

Figure 10. Comparing Superheat of R134a and R1234yf

Finally Fig. 10 shows the variation of superheat after the step perturbation. During the first 50 seconds the evaporator is operating at steady state and the level of superheat is constant for the R1234yf and R134a of 8.1 and 11.1 ° C, respectively. When t=50 s the mas flow rate at the evaporator inlet was reduced sharply and the amount of mass inside the evaporator decreases causing an increased in the superheat at the outlet of the evaporator. As seen in Fig. 10, R1234yf always has a degree of superheat lower than R134a. This occurs due to the difference between the evaporation latent heats of the two fluids. The time for the superheat stabilize for R1234y is also higher than for R134a. This occurs for the same reasons seen in Fig. 7 to 9.

7 CONCLUSION

In this work it was presented a mathematical model of an evaporator operating at steady state with R134a fluid. A total of 36 tests were performed for the validation. As can be seen the deviation decreases when the rotation is increased and the condensation temperature. The results show that the model can predict the evaporation temperature of ± 2 ° C with an error range when the evaporation temperature is above 0 ° C. However, new tests should be conducted to evaporation temperatures below this limit. In addition, a new validation for the rotation of 900 rpm.

A mesh test was performed after the model validation to determine the suitable number of elements to divided the evaporator. Several simulations were performed in steady state, with different numbers of elements (*n*). The minimum number of elements required for a consistent response with a variation of ± 0.2 ° C is 150 elements.

A comparison of thermal behavior of R134a and R1234yf was performed by numerical simulation of the evaporator operating in transient regime. During the simulations of mass flow rate reduction at the inlet of the evaporator, it was observed that the thermal resistance of R1234yf fluid is greater than that of R134a, because the heat transfer coefficient is less R1234yf throughout evaporator. It was also observed that the R1234yf the evaporation temperature is higher than the R134a because the latent heat of vaporization R1234yf is less than that of R134a.

8 ACKNOWLEDGEMENTS

Thanks to the support of the Graduate Program in Mechanical Engineering (PPGMEC) of the Federal University of Minas Gerais.

REFERENCES

Babiloni, A.M., Esbrí, J.N., Barragán, A., Molés, F. e Peris, B. Analysis based on EU Regulation No 517/2014 of new HFC/HFO mixtures as alternative of high GWP refrigerants in refrigeration and HVAC systems. International Journal of Refrigeration, vol. 52, p.21-31, 2015.

Babiloni, A.M., Esbrí, J.N., Barragán, A., Molés, F. e Peris, B. Drop-in energy Performance evaluation of R1234yf and R1234ze(E) in a vapor compression system as R134a replacements. Applied Thermal Engenieering, vol. 71, p.259-265, 2014.

Cho, H., Lee, H. e Park, C. Performance characteristics of an automotive air conditioning system with internal heat exchanger using refrigerant R1234yf. Applied Thermal Engineering, vol. 61, p.563-569, 2013.

Dinçer, I. and Kanoglu, M. Refrigeration Systems and Applications. 2ª Ed., United Kingdom, John Wiley & Sons, 464p, 2010.

Directive 2006/40/EC of the European Parliament and of the Council of 17 May 2006 relating to emissions from air conditioning systems in motor vehicles and amending Council Directive 70/156/EC. Off. J. Eur. Union, 2006.

Esbrí, J.N, Miranda, J.M.M, Babiloni, A.M., Cervera, A.B. e Flores, J.M.B. Experimental analysis of R1234yf as drop-in replacements for R134a in a vapor compression system. International Journal of Refrigeration, vol. 36, p.870-880, 2013.

Esbrí, J.N,, Cervera, A.B. e Molés, F. Experimental analysis of the internal heat exchanger influence on a vapour compression system performance working with R1234yf as drop-in replacement for R134a. Applied Thermal Enginerring, vol. 59, p.153-161, 2013.

Higashi, Yukihiro and Meisei Iwaki. "Thermophysical properties of HFO1234yf and HFO1234ze(E)" (2010) International Symposium on Next-generation Air Conditioning and Refrigeration Technology, 17 – 19 February 2010, Tokyo, Japan

Incropera, F.P., Dewitt, D.P., Bergman, T.L., Lavine, A.S. Fundamentos de Transferência de Calor e Massa. 6ª Ed., Rio de Janeiro, LTC, 644p, 2008.

Kyoto Protocol, Report of the Conference of the Parties, United Nations Framework Convention on Climate Change (UNFCCC), New York, USA, 1997.

Koury, R.N.N. Modelagem numérica de uma máquina de compressão de vapor. Tese de Doutorado. Faculdade de Engenharia Mecânica, Universidade Estadual de Campinas, Campinas, 112p., 1998.

Lee, Y. e Jung, D. A brief performance comparison of R1234yf and R134a in a bench tester automobile applications. Applied Thermal Engineering, vol. 35, p.240-242, 2012.

Li, H., Cao, F., Bu, X., Wang, L. e Wang, X. Performance characteristics of R1234yf ejector-expansion refrigeration cycle. Applied Energy, vol. 121, p.96-103, 2014.

Machado, L. Modele de simulation et etude experimentale d'un evaporateur de machine frigorifique em regime transitoire. Thèse de Doctorat, INSA, Lyon, France, 160p., 1996.

Miranda, J.M., Minguela, J.J., Carpio, V.D. e Esbrí J.N. Development and Validation of a micro-fin Tubes evaporador model using R134a and R1234yf as working fluids. Interenational Journal Rerigeration, vol. 50, p.32-43, 2015.

Molés, F., Esbrí, J.N., Peris, B., Babiloni, A.M. e Cervera, A.B. Theoretical energy performance evaluation of different single stage vapour compression refrigeration configurations using R1234yf and R1234ze(E) as working fluids. International Journal of refrigeration, vol. 44, p.141-150, 2014.

Ozisic, M.N. Heat Transfer, a basic approach. New York, MacGraw-Hill, 780p., 1985.

Reasor, Pamela, Aute, Vikrant, e Radermacher, Reinhard, "Refrigerant R1234yf Performance Comparison Investigation" (2010). International Refrigeration and Air Conditioning Conference. Paper 1085.

Regulation (EU) No 517/2014 of the European Parliament and the Council of 16 April 2014 on fluorinated greenhouse gases and repealing Regulation (EC) No 842/2006. Off. J. Eur. Union, 2014.

Rice, C.K. The effect of void fraction correlation and heat flux assumption on refrigerant charge inventory preditions. ASHRAE Transactions, vol. 93, Part. 1, p. 341-367, 1987

Turaga, M., Guy, R.W., Rupta, C.P. Refrigerant side heat transfer and pressure drop estimates for direct expansion coils. A review of works in North American use. Int. Journal Refrigeration, vol. 8, p. 134-142, 1985.

United Nations Environment Program (UNEP), Montreal Protocol on Substances that Deplete the Ozone Layer, 1997 (Final Act, United Nations, New York, USA.

Zilio, C., Brown, J.S., Schiochet, G. e Cavallini, A. The refrigerant R1234yf in air conditioning systems. Energy, vol. 36, p.6110-6120, 2011.